Arch. Metall. Mater. **65** (2020), 3, 1011-1014

DOI: 10.24425/amm.2020.133208

JUN HYUK JUNG[1], JIWON HONG[1], YOUNGRYEUL KIM[1],
SEOK-MIN YONG[1], JINWOO PARK[1], SEUNG JUN LEE[1*]

ELECTROTHERMAL PROPERTIES AND RF TRANSMITTANCE OF SPRAY-COATED CNT THIN FILM FOR RADOME DE-ICING APPLICATION

Ice formed on radome surfaces causes communication disruption due to radio-frequency interference (RFI), which reveals the importance of de-icing systems for radomes. As a radome de-icing application, in this work, carbon nanotube (CNT) thin films were fabricated using a spray-coating method, and influence of process parameters on RF transmittance and electrothermal properties was investigated. With the increase of spraying time, sheet resistance of the fabricated film decreases, which results in a decrease of the RF transmittance and improvement of the heating performance. Also, the de-icing capability of the fabricated CNT film was evaluated at –20ºC, and efficient removal of ice under cold conditions was demonstrated.

Keywords: De-icing, CNT thin film, spray-coating, electrothermal property, RF transmittance

1. Introduction

In the aviation industry, the need to improve all-weather flying safety is important [1]. Especially, radomes, protecting covers for radar devices in aircraft, should exhibit good radar performance even under hostile environments. In aviation at high altitude, however, ice can easily form on radome surfaces and may cause significant communication failures of the radar system. Therefore, a number of studies have reported ice removal methods to protect radome surfaces from ice accumulation [2-6]. One promising de-icing method is to use Joule heating of a conductive heating film coated on the radome surface.

The materials most commonly used as conventional conductive heating films are transparent conducting oxides (TCO) such as indium-doped tin oxide (ITO), fluorine-doped tin oxide (FTO), and aluminum-doped zinc oxide (AZO). Generally, TCOs show high optical transmittance and high electrical conductivity [7,8]. However, because of its brittle nature and complex processing, along with expensive cost, TCOs do not seem feasible for use as radome heating materials. To overcome the limitations of TCO thin films, carbon nanotubes (CNTs) have been considered as alternative material for conductive heating films in recent studies [2,6]. Compared with TCOs, CNTs have many advantages, including low cost, excellent inherent electrical properties, ease of solution-based processing, and chemical stability [9].

There are a variety of fabrication methods for making CNT thin films: dip coating [10], brush painting [11], rod coating [12], spin coating [13], spray-coating [14], vacuum filtration [15], and electrophoretic deposition [16]. However, CNT films for radome de-icing should cover large-size curved surfaces. In contrast to other coating methods, spray coating has advantages in large-scale fabrication of conductive films on curved surfaces, as well as in simple conditions and ease of processing.

In this study, we fabricated CNT conductive thin films using a spray coating method. For application of this material as a radome de-icing film, we investigated the effects of process parameters on electrothermal performance and RF transmittance.

2. Experimental

0.45 mg of MWCNTs (CM-150, Hanwha Chemical. Republic of Korea) and an identical weight of sodium dodecyl benzene sulfonate (SDBS) as surfactant were added to 300 mL of distilled water for preparation of 0.15 wt.% MWCNT aqueous solution. Then, the mixture was sonicated using a probe ultrasonicator (VCX 750, Sonics & Materials, USA) for 90 min with 60% amplitude.

Using a spray gun with a nitrogen flow of 4 MPa back pressure, the MWCNT aqueous solution was spray-coated on a glass

[1] AGENCY FOR DEFENSE DEVELOPMENT (ADD), YUSEONG P.O. BOX 35, DAEJEON 34186, REPUBLIC OF KOREA

* Corresponding author: keramos99@gmail.com

substrate (22.8 mm × 10.1 mm). During the spraying process, the glass substrate was put on a hot plate preheated to 180°C. Spray distance was fixed 90 cm from the hot plate. The spraying time was varied from 30 to 240 sec. The fabricated CNT films are denoted as CNT X for spraying time X seconds. A summary of the electrical and electrothermal properties, and of the transmittance of the fabricated CNT films, is shown in Table 1.

TABLE 1

Summary of electrical and electrothermal properties, and transmittance of fabricated CNT films

Sample	Spraying Time (sec)	R (kΩ)	R_{sh} (kΩ/□)	Response Time at 60V (sec)	$T_{steady\text{-}state}$ at 60V (°C)	Transmittance at 10 GHz (%)
CNT 30	30	15.80	8.18	34.0	53.8	92
CNT 60	60	4.59	2.44	28.2	113.6	84
CNT 90	90	2.70	1.47	25.9	151.4	76
CNT 120	120	2.29	1.19	28.4	166.2	74
CNT 180	180	1.93	1.00	21.7	181.7	70
CNT 240	240	1.55	0.80	19.5	200.1	66

The electrical linear resistance (R) of each specimen was measured using a Keithely sourcemeter (2612A, Keithely, USA). The sheet resistance (R_{sh}) of the conductive films was calculated by the following *equation*, $R_{sh} = R \times (W/L)$, where R is the electrical linear resistance, W is the width, and L is the length. Using a Network Analyzer (PNA N5222A, Keysight, USA), the radio frequency (RF) transmittance was measured in the range of the X-band (8.2-12.4 GHz). The heating performance of the films was tested with a thermal imaging camera (A35, FLIR Systems, USA), in real time, by applying DC voltage from 20 to 60 V for 4 min. For the de-icing performance test, a sample with a droplet of water on the film surface was put into a temperature and humidity chamber (EN-STH-604, ENEX Science, Republic of Korea) at –20°C. After the water completely froze, ice and ambient temperature were recorded using a thermal imaging camera with applying DC voltage.

3. Results and discussion

Figure 1 shows the sheet resistance (R_{sh}) as a function of the spraying time. As the spraying time increased from 30 to 240 sec, R_{sh} decreased from 8.18 to 0.80 kΩ/□ (Table 1). For the spray-coating process, generally, density and thickness of fabricated film increase as the spraying time increases. The increase of the density and thickness of the fabricated CNT film means that the connectivity of the MWCNTs was improved [17]. The inset in Fig. 1 provides photograph and SEM images of CNT 30, CNT 90, and CNT 240. The SEM micrographs show two different regions, i.e. dark and bright regions, which correspond to CNT-coated and uncoated (bare glass) region, respectively. As shown in the inset of Fig. 1, these results match well with the decrease of optical transparency (optical images) and the reduction of the uncoated region (SEM images) according to the increase of spraying time.

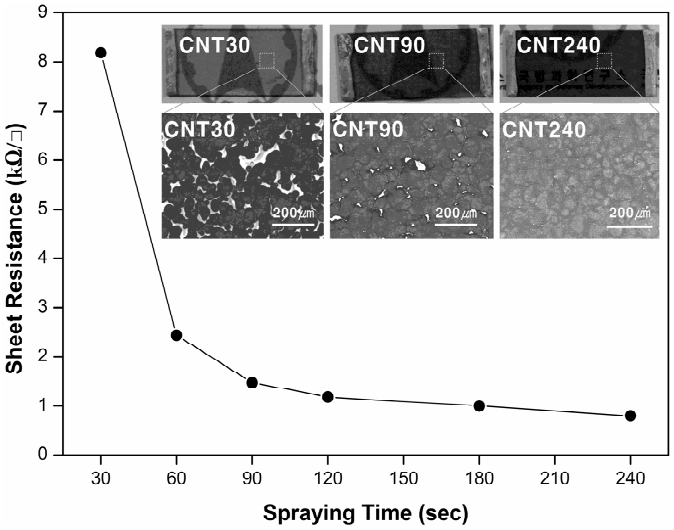

Fig. 1. Sheet resistance as a function of spraying time. Photo and SEM images of CNT films on glass substrate are shown in inset

Figure 2(a) shows the RF transmittance of the specimen in the range of the X-band as linearly transformed from the measured S-parameter (dB). Although the transmittance decreases at low frequency due to waveguide (WR-90) loss [18], it was confirmed that all samples have somewhat linear characteristics, with transmission difference of less than 10% in all ranges. Fig. 2(b) displays the RF transmittance at 10 GHz as a function of spraying time. CNT 30 exhibited the highest RF transmittance of 92%; as the spraying time increased to 240 sec, the RF transmittance decreased to 66% (Table 1). This phenomenon can be explained by the transmission line theory, which defined the relation between conductivity and electromagnetic (EM) wave transmission [18].

$$T = \frac{2Z_1}{Z_0 + Z_1} \tag{1}$$

where T is the transmission coefficient and Z_0 is the free-space impedance. The medium impedance (Z_1) is calculated according to

$$Z_1 = \sqrt{\frac{j\omega\mu}{\sigma + j\omega\varepsilon}} \tag{2}$$

where σ is the conductivity of the medium, ω is the angular frequency of the wave, and ε and μ are the permittivity and permeability, respectively. As spraying time increased, the CNT content, which is related to ε and σ, increased, and this leads to a decrease in EM wave transmittance.

Figure 3(a) presents the time-dependent temperature changes of CNT 60 under constant applied voltages of 20, 40, and 60 V. Regardless of the applied voltage, the temperature increases rapidly to a maximum value within 100 sec when certain voltage is applied. The response times [19], which is defined as the time to reach approximately 90% of the steady-state temperature ($T_{steady\text{-}state}$) from room temperature, increase to 17.0, 21.1, and 28.2 sec with increasing applied voltage. $T_{steady\text{-}state}$ remains unchanged over the applied voltage, and decreases to

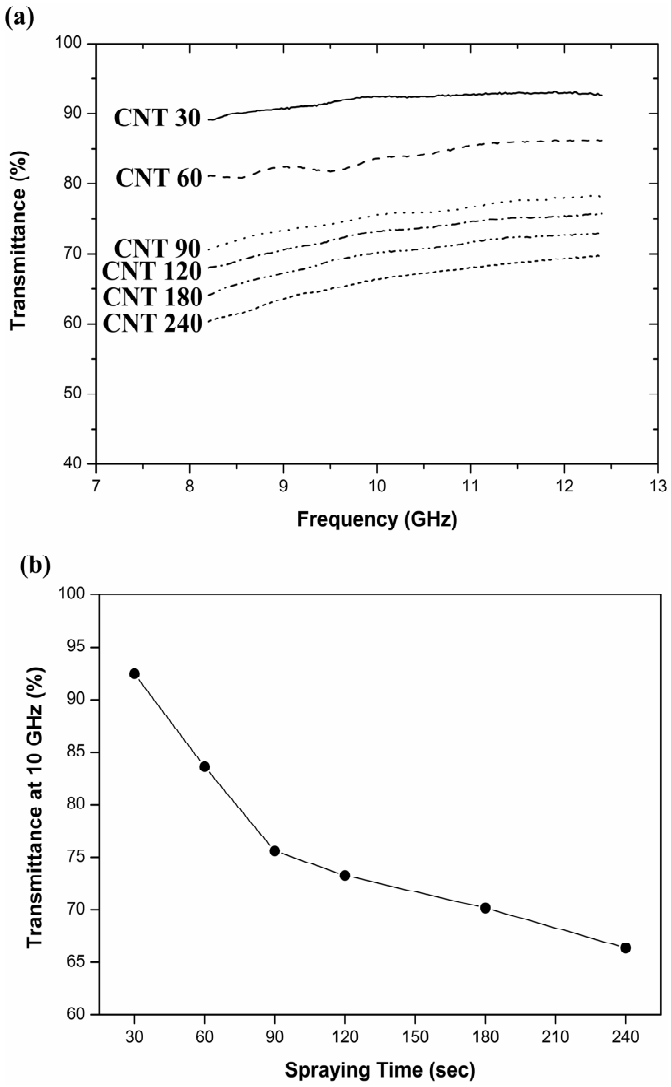

Fig. 2. (a) X-band transmittance of specimens, (b) RF transmittance at 10 GHz as a function of spraying time

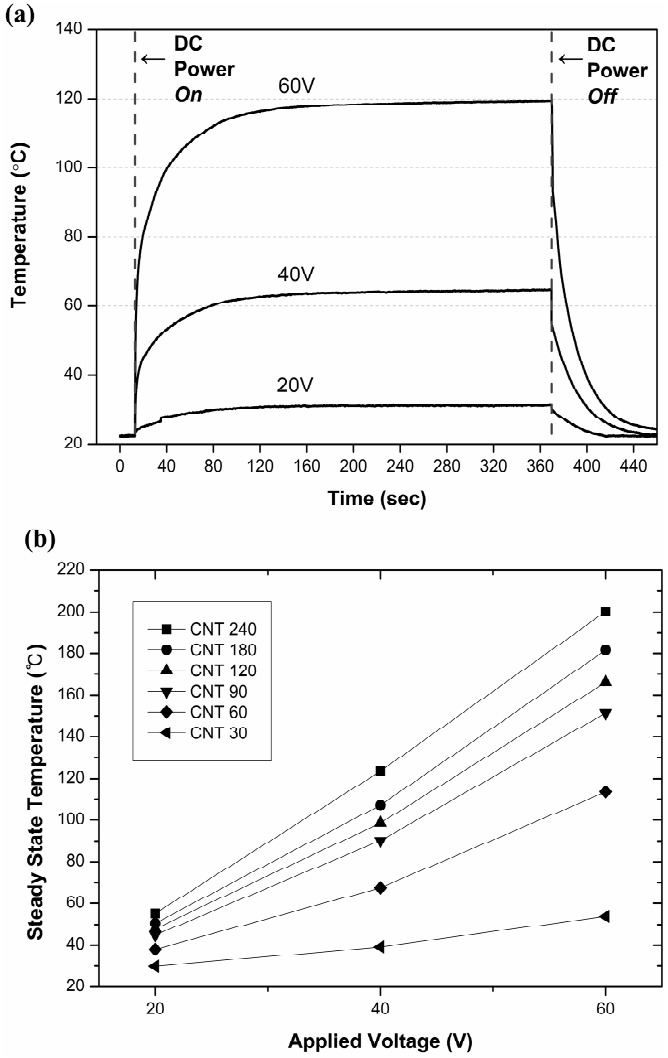

Fig. 3. (a) Time-dependent temperature changes of CNT 60 under constant applied voltage, (b) Steady state temperature of fabricated CNT films under different constant voltages

room temperature when the applied voltage is off. This electric heating behavior of the fabricated CNT film is found to be strongly dependent on the spraying time as well as the applied voltage. $T_{steady\text{-}state}$ of the fabricated CNT films under different constant voltages are illustrated in Fig. 3(b). $T_{steady\text{-}state}$ values are found to increase with the increase of the spraying time and applied voltage, which can be explained by the relationship of $P = IV = V^2/IR$, where P is the electrical power, I is the current, V is the voltage, and R is the resistance, i.e. , the electric power is converted to heat by resistance heating or Joule heating process in the CNT films [17].

Figure 4(a) shows the time-dependent temperature change profile of CNT 60 at –20°C. $T_{steady\text{-}state}$ was reached within 100 sec of applying voltage, and increased to –8, 25, and 81°C when the applied voltage increased to 20, 40, and 60 V, respectively. In comparison with the results shown in Fig. 3(a), it was confirmed that the temperature difference from initial temperature to $T_{steady\text{-}state}$ does not change, which reveals that the fabricated CNT films exhibit an inherent Joule heating characteristic regardless of the ambient temperature. However, it was confirmed that the response time varies depending on the ambient temperature. The response time at room temperature was 17-29 sec, but the response time increased to 42-51 sec at –20°C. This can be attributed to the low temperature and strong convection in the temperature chamber. To demonstrate the deicing performance, a CNT 60 sample with a water droplet was placed in the temperature chamber at –20°C. After the water droplet froze, DC 40 V was applied to the CNT film until the ice melted completely; at the same time, the temperatures of the ice and water were measured. The results are shown in Fig. 4(b). The time-dependent temperature change curve of ice and water can be divided into three stages. In the first stage, the temperature of ice rapidly increased to 0°C during less than 50 sec. In the second stage, the temperature of ice was fixed at approximately 0°C until completion of the phase change of ice to water, which took about 300 sec. This was because the generated thermal energy of the CNT film was transformed into latent heat of ice. As shown in the third stage in Fig. 4(b), after the phase change of ice, the temperature of the water increased to $T_{steady\text{-}state}$ with lower heating rate than that of the first stage. Images of ice be-

fore applying voltage and after completely melting are shown in Fig. 4(c). Based on these results, it was confirmed that CNT films exhibits de-icing performance even in a hostile environment of –20ºC.

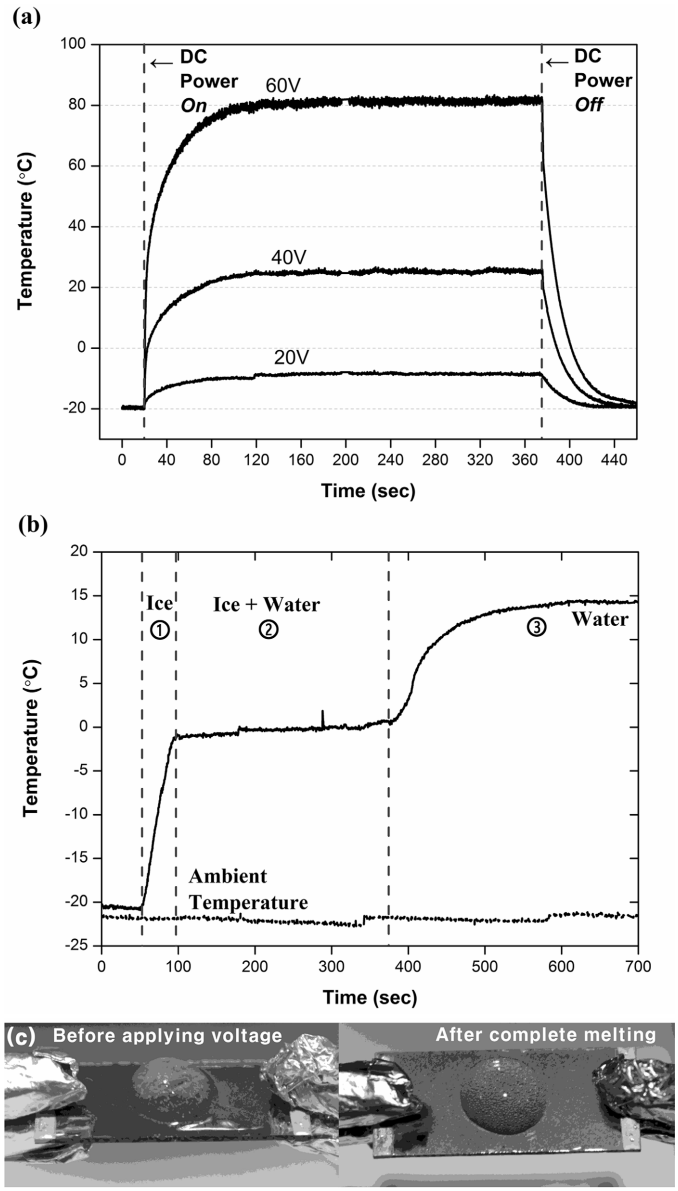

Fig. 4. (a) Time-dependent temperature change profile of CNT 60 at –20ºC, (b) Time-dependent changes of ice and ambient temperature under constant applied voltage of 40 V for CNT 60, (c) Images of ice before applying voltage and after complete melting

4. Conclusions

In this study, the influence of the spraying time on the RF transmittance and electrothermal properties of CNT films fabricated using spray-coating method was investigated. It was found that RF transmittance decreases and heating performance improves with increasing spraying time. This was attributed to the decrease of sheet resistance of the fabricated CNT film due to improvement of connectivity of the MWCNTs network. It was demonstrated that spray-coated CNT films with RF transmittance of 84% at 10 GHz exhibit effective de-icing capability at –20ºC. Based on the above results, it is expected that, with modification and optimization of the process parameters, these spray-coated CNT films can be used for radome de-icing applications.

Acknowledgments

This work was supported by DAPA and ADD.

REFERENCES

[1] L.S. Groff, J.M. Price, Aviat. Space Environ. Med. **77** (10), 1062-1067 (2006).
[2] X. Yao, S.C. Hawkins, B.G. Falzon, Carbon **136**, 130-138 (2018).
[3] K.L. Sørensen, A.S. Helland, T.A. Jahansen, IEEE Aero. Conf. 1-6 (2015).
[4] O. Redondo, S.G. Prolongo, M. Campo, C. Sbarufatti, M. Giglio, Compos. Sci. Technol. **164**, 65-73 (2018).
[5] V. Volman, Y. Zhu, A.-R. O. Raji, B. Genorio, W. Lu, C. Xiang, C. Kittrell, J. M. Tour, ACS Appl. Mater. Interfaces **6**, 298-304 (2014).
[6] J. Luo, H. Lu, Q. Zhang, Y. Yao, M. Chen, Q. Li, Carbon **110**, 343-349 (2016).
[7] D.-J. Kwak, B.-H. Moon, D.-K. Lee, C.-S. Park, Y.-M. Sung, J. Elec. Eng. Technol. **6** (5), 684-687 (2011).
[8] R.A. Afre, N. Sharma, M. Sharon, M. Sharon, Rev. Adv. Mater. Sci. **53**, 79-89 (2018).
[9] L. Yu, C. Shearer, J. Shapter, Chem. Rev. **116**, 13413-13453 (2016).
[10] F. Mirri, A.W.K. Ma, T.T. Hsu, N. Behabtu, S.L. Eichmann, C.C. Young, D.E. Tsentalovich, M. Pasquali, ACS Nano **6** (11), 9737-9744 (2011).
[11] D.-Y. Cho, K. Eun, S.-H. Choa, H.-K. Kim, Carbon **66**, 530-538 (2014).
[12] Y. Meng, X.-B. Xu, H. Li, Y. Wang, E.-X. Ding, Z.-C. Zhang, H.-Z. Geng, Carbon **70**, 103-110 (2104).
[13] H.-S. Jang, S.-K. Jeon, S.-H. Nahm, Carbon **49**, 111-116 (2011).
[14] V.H. Pham, T.V. Cuong, S.H. Hur, E.W. Shin, J.S. Kim, J.S, Chung, E.J. Kim, Carbon **48**, 1945-1951 (2010).
[15] Z. Wu, Z. Chen, X. Du, J.M. Logan, J. Sippel, M. Nikolou, K. Kamaras, J.R. Reynolds, D.B. Tanner, A.F. Hebard, A.G. Rinzler, Science **305** (5688), 1273-1276 (2018).
[16] S. Pei, J. Du, Y. Zeng, C. Liu, H.-M. Cheng, Nanotechnology **20**, 235707 (2009).
[17] D. Jung, M. Han, J. Vac. Sci. Technol. B **32**, 04E105 (2014).
[18] D.M. Pozar, Microwave Engineering, Wiley (2011).
[19] D. Sui, Y. Huang, L. Huang, J. Liang, Y. Ma, Y. Chen, Small **7**, 3186-3192 (2011).